(2)

ANOMALOUS STRAIN RATE DEPENDENCE OF THE SERRATED FLOW IN Ni - H AND Ni - C - H ALLOYS

A. KIMURA AND H. K. BIRNBAUM

UNIVERSITY OF ILLINOIS
DEPARTMENT OF MATERIALS SCIENCE & ENGINEERING

TECHNICAL REPORT

SEPTEMBER 1989

OFFICE OF NAVAL RESEARCH

USN 00014-83-K-0468

Unclassified

SECURITY CLASSIFICATION OF THIS PAGE (When Data Entered)

REPORT DOCUMENTATION PAGE		READ INSTRUCTIONS BEFORE COMPLETING FORM
1. REPORT NUMBER	2. GOVT ACCESSION NO.	3. RECIPIENT'S CATALOG NUMBER
4. TITLE (and Subtitle) Anomalous Strain Rate Dependence of the Serrated Flow in Ni-H and Ni-C-H Alloys		5. TYPE OF REPORT & PERIOD COVERED Technical Report 9/89 6. PERFORMING ORG. REPORT NUMBER
7. AUTHOR(s) A. Kimura and H.K. Birnbaum		8. CONTRACT OR GRANT NUMBER(s) USN00014-83-K-0468
9. PERFORMING ORGANIZATION NAME AND ADDRESS Dept. of Materials Science & Engineering Univ. Of Illinois Urbana, IL 61801		10. PROGRAM ELEMENT, PROJECT, TASK AREA & WORK UNIT NUMBERS
11. CONTROLLING OFFICE NAME AND ADDRESS Office of Naval Research 100 N. Quincy Arlington, VA		12. REPORT DATE September 1989 13. NUMBER OF PAGES 24
14. MONITORING AGENCY NAME & ADDRESS(if different from Controlling Office)		15. SECURITY CLASS. (of this report) Unclassified 15a. DECLASSIFICATION/DOWNGRADING SCHEDULE

16. DISTRIBUTION STATEMENT (of this Report)

This document is unclassified. Reproduction and distribution of this document for any purpose of the U.S. government is permitted.

17. DISTRIBUTION STATEMENT (of the abstract entered in Block 20, if different from Report)

18. SUPPLEMENTARY NOTES

19. KEY WORDS (Continue on reverse side if necessary and identify by block number)

Nickel
Nickel alloys
Hydrogen
Serrated flow
Portevin-LeChatalier effect
Dislocations

20. ABSTRACT (Continue on reverse side if necessary and identify by block number)

Serrated flow in Ni-H, Ni-C-H, and Ni-C alloys was studied over a wide range of temperature and strain rates. The results for C related serrated flow in Ni-C or Ni-C-H alloys were in excellent agreement with previous results and were consistent with dislocation pinning by C solutes at the dislocation cores. Hydrogen related serrated yielding was observed in Ni-H and Ni-H-C alloys. Solute C had only a small effect on the temperature range of this H related serrated flow. The results could be interpreted on the basis of hydride formation at the dislocation cores and diffusion of H in these hydrides.

DD FORM 1 JAN 73 1473 EDITION OF 1 NOV 65 IS OBSOLETE
S/N 0102-LF-014-6601

Unclassified

SECURITY CLASSIFICATION OF THIS PAGE (When Data Entered)

Anomalous Strain Rate Dependence of the Serrated Flow in Ni-H and Ni-C-H Alloys

A. Kimura and H.K. Birnbaum
Department of Materials Science and Engineering
University of Illinois at Urbana-Champaign
Urbana, IL 61801

ABSTRACT

Serrated flow in Ni-H, Ni-C-H, and Ni-C alloys was studied over a wide range of temperature and strain rates. The results for C related serrated flow in Ni-C or Ni-C-H alloys were in excellent agreement with previous results and were consistent with dislocation pinning by C solutes at the dislocation cores. Hydrogen related serrated yielding was observed in Ni-H and Ni-H-C alloys. Solute C had only a small effect on the temperature range of this H related serrated flow. The results could be interpreted on the basis of hydride formation at the dislocation cores and diffusion of H in these hydrides.

MRL-88-0007

I. INTRODUCTION

It is well known that serrated flow in alloys can be caused by dynamic strain aging (1,2) during the deformation process. Since this process implies that solute atoms must be able to diffuse with or to the moving dislocations, the process is sensitive to temperature and strain rate and the regime in which serrations appear is generally bounded by lower and upper critical temperatures at each strain rate. The activation enthalpy for the lower critical temperature is equal to that for the solute diffusion in b.c.c. interstitial alloys, e.g. Fe-(C+N) (3) and V-(C+O) (4), while the activation enthalpy which characterizes the upper critical temperature has not yet been related to a physical process. Kinoshita et al (3) suggested that the activation enthalpy for the upper critical temperature equals (Q_D + ΔE) where Q_D is the activation enthalpy for solute diffusion and ΔE is the binding enthalpy of the solute to the dislocations. This interpretation was challenged by Yoshinaga et al (41) who showed that the apparent activation enthalpy for the upper critical temperature in V-(O+C) alloys was anomalously high, 3.3 eV. (Q_D of carbon or oxygen in vanadium is about 1.2 eV.)

In f.c.c. substitutional alloys, the activation energy for the initiation of the serrations has been obtained from the temperature dependence of the critical strain at which serrations appear on the stress strain curve. In Cu-Sn alloys the activation energy so determined is in good agreement with that for vacancy motion in the alloy (5). In Al-Mg alloys, however, the activation enthalpy obtained in this manner does not agree with that for the motion of a single vacancy (6) and the discrepancy has been explained by suggesting that diffusion may occur by the motion of di-vacancies (7,8) or attributed to a binding enthalpy between vacancies and solute atoms (9).

In nickel alloys, serrated flow has been investigated for Ni-C and Ni-H interstitial alloys. In Ni-C alloys (10) the lower critical temperature had an activation enthalpy of about half that of bulk diffusion of carbon and was associated with diffusion of carbon in the dislocation core. The binding enthalpy of carbon atoms to dislocations was estimated from the upper critical temperature to be about 0.5 eV from the assumption that the activation enthalpy was (Q_D + ΔE). It was also observed that serrations were not affected by quenched-in vacancies. Serrated flow in hydrogen charged nickel has been studied by Smith et al. (11-13) and Blakemore (14,15). The activation enthalpies obtained from these two studies differed greatly; being 0.27 eV and 1.74 eV for the lower and upper critical temperatures in the work by Smith et al. (13) and 0.59 eV and 0.71 eV in the work by Blakemore (14). Their mechanistic interpretations also differed; Smith et al (13) associating the lower activation enthalpy with bulk hydrogen diffusion and Blakemore et al (14) with a trapping effect at vacancies or grain boundaries. The anomalously high value of the activation enthalpy for the upper critical temperature obtained by Smith et al. (13) was accounted for by the dissipation of the hydrogen atmosphere at dislocations.

The present study examines serrated flow in Ni-H and Ni-C-H alloys over a wide range of strain rates. A mechanism of serrated flow in Ni-H and Ni-C-H alloys is proposed based on the experimental results.

II. EXPERIMENTAL METHODS

High purity nickel wire (1mm diameter) of 99.999% nominal purity was annealed in purified hydrogen gas at 1173 K for 3 days to remove interstitial impurities. Carburization was carried out by annealing in gaseous 95% CO-5%CO_2 mixtures at 1223 K for 2 days followed by quenching into oil. Both

purified and carburized nickel was simultaneously charged with hydrogen by annealing in hydrogen gas at 1073 K for 5 min followed by quenching into oil. The results of chemical analysis of the specimens after preparation are shown in Table I with the H concentration determined by hot vacuum extraction. The same amount of hydrogen was present in both nickel and nickel carbon alloys. The average grain size was determined to be about 150 micrometers for both materials. Tensile tests were carried out at strain rates from 4.4×10^{-3} s^{-1} to 2.8×10^{-7} s^{-1} at test temperatures which were controlled to $\pm$ 0.2 degrees.

Previous studies (14) indicate, the critical temperatures are strongly dependent on the hydrogen concentration. In the present study it was also found that the critical temperatures often differed among nominally identical specimens and experimental conditions suggesting that even small changes in hydrogen concentration affect the critical temperatures. Therefore in this study, the critical temperatures were determined by a procedure which allowed a complete determination on a single specimen. The specimen was deformed at a given temperature to determine whether serrated flow occurred and then was unloaded. After changing the deformation temperature by a few degrees, the specimen was reloaded with the same strain rate and any serrated yielding was observed. This procedure was continued until a total strain of 2% was achieved. This upper strain limit minimized the effect of strain on the appearance of serrations. In Ni-H alloys, the serrations appeared almost immediately after yielding and continued up to large strains (more than 10%) near the lower critical temperatures. Near the upper critical temperatures serrated yielding disappeared after a few percent strain. To determine whether the cause of the disappearance of serrations was temperature or strain, the presence of serrations was always reconfirmed by the last test of each series at a suitably low temperature.

III. EXPERIMENTAL RESULTS

1. Serrated Flow in Ni-H Alloys

A typical series of stress-strain curves of Ni-270 at ppm H alloys deformed at two different strain rates at temperatures near the lower critical temperature is shown in Fig. 1. As shown, the appearance of serrations in the flow region depended critically on the deformation temperature. The Lüders deformation and the yield point phenomena observed during most tests were probably caused by static strain aging between tests during changes of the deformation temperature. Figure 2 shows the serrated flow in Ni-H alloys at temperatures near the upper critical temperature at relatively high strain rates. Serrated flow was not observed above 228K for relatively high strain rates (curves A and C are for 1.2×10^{-5} s^{-1} and B is for 4.4×10^{-4} s^{-1}). This independence of the upper critical temperature on strain rate is confirmed at much slower strain rates as shown in Fig. 3. At a strain rate of 1.8×10^{-6} s^{-1} the upper critical temperature is 226 K. The three stress-strain curves shown at the bottom of this figure are at a strain rate of 2.8×10^{-7} s^{-1} for which serrated flow was observed at 220 K and 224 K but not at 228 K. (The small steps observed at this low strain rate are artifacts of the tensile machine when operated at this very low crosshead speed.)

Figure 4 shows the serrated flow region of Ni-270 at ppm H alloys as a function of deformation temperature and strain rate. Two anomalous behaviors were observed; first, a marked discontinuity was observed in the slope of the lower critical temperature line. A fit of the Arrhenius expression to the data yields an activation enthalpy of 0.25 eV at the higher strain rates and 0.57 eV at the lower strain rates. Both values differ significantly from that for hydrogen diffusion in nickel; 0.41 eV (16). The 0.25 eV obtained at the higher strain rates is in excellent

agreement with the value obtained by Smith et al (13) and the value of 0.57 eV at low strain rates agrees with Blakemore (14,15); thus resolving this disagreement. A second anomalous behavior is that the upper critical temperature does not depend on the strain rate; which suggests that this temperature is not determined by a mechanism involving hydrogen interactions with moving dislocations. This result is not inconsistent with the very high activation enthalpies previously reported (12,13).

2. Serrated Flow in Ni-C Alloys

The temperature-strain rate diagram for Ni-5100 at ppm C alloys is shown in Fig. 5. This data is in good agreement with previous results (10) as are the activation enthalpies which characterize the lower critical temperatures (0.62 eV) and the upper critical temperature (1.14 eV).

3. Serrated Flow in Ni-C-H Alloys

A typical series of stress-strain curves of Ni-5050 at ppm C-270 at ppm H alloys deformed at a strain rate of 4.4×10^{-5} s^{-1} at temperatures between 228 and 254 K is shown in Fig. 6. Serrated flow was observed below 233 K and above 245 K. Figure 7 shows the temperature-strain rate diagram for this alloy and the comparison with that of the Ni-C and Ni-H alloys. The Ni-C-H alloys show serrated flow in two distinct temperature regimes. In the lower temperature range the serrated flow has upper and lower bounds at somewhat higher temperatures than for Ni-H alloys. In the higher temperature range the upper and lower bounds are in excellent agreement with those for the Ni-C alloy. At strain rates of about 10^{-3} s^{-1} a region where no serrations were seen separates the two regions of serrations; at lower strain rates the two regions overlap. Direct comparison of the

results for the Ni-C-H alloys with those of the Ni-C and Ni-H alloys suggest that at lower temperatures the serrations are caused by hydrogen solutes while at higher temperatures they are associated with carbon solutes.

4. Effect of Serrated Flow on the Work-hardening Rate

Figure 8 shows the work-hardening rates of Ni, Ni-H, Ni-C and Ni-C-H alloys at 295, 198 and 77 K at a strain rate of 4.1×10^{-5} s^{-1}. All of the work-hardening rates increase as the temperature is decreased. Hydrogen causes a small increase of the work-hardening rate in pure Ni at 198K and 295K and has little effect on the work-hardening of Ni-C alloys. There was no effect of hydrogen on either alloy at 77 K. Since serrated yielding and work hardening in the Ni-H alloys may both be related to dislocation -H interactions, the flow stresses of Ni-H alloys were compared before and after outgassing of hydrogen at 473 K for 2 hr with the typical results shown in Fig. 9. At 198 K, where hydrogen causes serrations, the flow stress decreased by 20 MPa after outgassing of hydrogen after a strain of about 0.1 while no significant change in flow stress due to H outgassing after a strain of 0.1 was observed at 295 K. These results are consistent with the increased work hardening and flow stress being due to changes in the dislocation configurations produced during deformation at 295 K and to H "pinning" of dislocations during deformation at 198 K. Removal of H by outgassing during an interrupted stress strain experiment in Ni-C-H alloys had no effect on the flow stress but did remove the low temperature serrated flow associated with H.

IV. DISCUSSION

In the preceding section it was shown that two distinct regions of "serrated flow" are observed for Ni-C-H alloys and that the effects of C and H on the

serrated yielding of Ni are in fact rather separate, ie. the parameters which characterize the $\dot{\varepsilon}$ - T region of serrated flow for Ni-H and for Ni-C alloys separately are not significantly different than those which describe the situation for Ni-C-H alloys. The principal exception to this is that the "upper and lower critical temperatures" for the serrated flow due to H are increased slightly by the presence of C in solid solution. The principle experimental observations which need to be discussed are:

a. serrated flow caused by H and C in Ni appear to be relatively distinct phenomena

b. The two branches of the "lower critical temperature" for the Ni-H system (Fig. 4) which are characterized by two Arrhenius relations between the strain rates, $\dot{\varepsilon}$, and the "lower critical temperatures", $T_{l.c.}$. The two activation enthalpies which characterize the branches are 0.57 eV at the lower strain rates and 0.25 eV at the higher strain rates; neither of which equals the H diffusion enthalpy in the Ni lattice.

c. The "upper critical temperatures" for the Ni-H system are independent of the strain rates in contrast to those of the Ni-C system (Figs. 4 and 7).

d. Hydrogen has a negligible effect on the work hardening rates of Ni-C alloys and on Ni at 77 K (Figs. 8 and 9). A small increase of the work hardening rate of Ni at about 200 and 295 K is found in Ni-H alloys.

e. The increased work hardening rate at 295 K due to H appears to be caused by permanent changes in the dislocation configuration, ie. it is unaffected by H outgassing during deformation (Fig. 9) while at 198 K much of work hardening is reversible on outgassing the H during deformation.

Serrated flow can be accounted for on the basis of dynamic strain aging as first proposed by Nabarro (17). Intermittent pinning of dislocations by solute atmosphere formation occurs at dislocation velocities below v_c described (18) by

$$v_c = 4D / R$$

where D is the solute diffusivity (lattice or dislocation core) which controls the formation of the solute atmosphere, $R = \beta / kT$ is the "effective radius" of the atmosphere, and β measures the strength of the dislocation - solute interaction. This dislocation velocity can be related to a "critical strain rate", $\dot{\varepsilon}_c$, given by

$$\dot{\varepsilon}_c = \rho b v_c = 4 b \rho D k T / \beta$$

where ρ is the mobile dislocation density and b is the Burgers vector. In this model serrated flow occurs by the repeated formation of solute atmospheres and the subsequent "breaking away" of the dislocations from these atmospheres. The principle parameters which determine the nature of the serrated yielding are the appropriate diffusivity and the interaction parameter, β. Serrated flow occurs at $T > T_{l.c.}(\dot{\varepsilon})$ above which the kinetics of atmosphere formation are favorable and at $T < T_{u.c.}$ determined by the temperature above which either the atmosphere no longer forms ($kT >> R/\beta$) or the temperature above which the atmosphere mobility is sufficiently high to allow it to drift with the dislocation, ie. no "breakaway" occurs.

In this model the Arrhenius temperature dependence of the $\ln \dot{\varepsilon}$ vs $T_{l.c.}$ is described by the enthalpy for the appropriate diffusion process. If the $T_{u.c.}$ is determined by the disappearance of the solute atmosphere, $T_{u.c.}$ is an effective

"solvus temperature" and is independent of the strain rate. Alternatively, if $T_{u.c.}$ is determined by the increased mobility of the atmosphere, the behavior is described by an Arrhenius temperature dependence with the activation enthalpy (Q_D + E) (3) where Q_D is the diffusion activation enthalpy and E is the solute - dislocation interaction enthalpy.

Previous discussions of serrated yielding have been stated in terms of sclute atmospheres and have been described by Maxwellian statistics. In the case of metal-hydrogen systems dislocation pinning can result from the formation of solute atmospheres or from the formation of a hydride along the core of the dislocation (19). In the case of core hydride formation $T_{u.c.}$ would correspond to the effective solvus temperature of the hydride, and is strain rate independent. The $T_{l.c.}$would then be determined by hydrogen diffusion in the core hydride or in the precursor atmosphere in the dislocation core depending on the strain rates. At high strain rates hydride formation may not occur and the activation enthalpy characteristic of $T_{l.c.}$ would be dislocation core diffusion of hydrogen solutes. Thus the measured value of 0.25 eV which characterizes the $T_{l.c.}$ at high strain rates can be interpreted as due to hydrogen diffusion in the dislocation core. At low strain rates, the hydride formation may occur at dislocations and the measured 0.57 eV would correspond to hydrogen diffusion in the core hydride.

Hydride formation is not observed at temperatures near 295 K at the H/Ni concentrations used in the present experiments. However, the solvus temperatures in the Ni-H system are not known and such hydrides may occur at the lower temperatures; particularly in the dislocation stress field where the tensile stresses can stabilize the hydride relative to the solid solution (20). The shift in the solvus temperature due the local stress is given by:

$$\Delta T = - \frac{\sigma_{kk} \Delta V_{hydride}}{R(\ln \gamma + \ln c_H)}$$

where σ_{kk} is the spherical component of the local stress (= 0.1μ at the dislocation core), $\Delta V_{hydride}$ is the volume increase on forming the hydride from the solid solution per mole of Ni atoms ($\Delta V_{hydride} = 0.18\ \Omega$ where Ω is the molal volume of Ni), γ is the activity coefficient of H in solid solution, and R is the gas constant. Assuming an ideal solution of H in Ni it can be estimated that $\Delta T_s \approx 40$ K at the dislocation core. Thus hydrides may be expected to form at the dislocation cores in the solid solutions of the present experiments and at the low temperatures where the serrated flow is observed.

Under the conditions of the present experiments it may be expected that the presence of C solutes would decrease the hydrogen diffusivity due to trapping. The effect of this would be to increase the $T_{l.c.}$ as is observed (Fig. 7). The effect of C solutes on the $T_{u.c.}$ is more difficult to predict as it depends on the effect of C on the relative free energies of H in the solid solution and in the core hydride. While there are small effects of C on the serrated yielding due to H solutes, no effect of H on the serrated yielding caused by C is observed. This is consistent with the above model for the serrated yielding. Since the temperature region of the serrations due to C is much higher than that in which H causes serrations trapping effects on C diffusivity should be relatively small. A smaller fraction of the C atoms should be associated with H solutes in this higher temperature range. Since the jump frequency of the H is very much higher than that of the C atoms those C solutes which are associated with H atoms should not be significantly impeded in their diffusivity by the trapping.

V. CONCLUSIONS

Investigation of serrated yielding in Ni-H and Ni-C-H alloys have shown that:

1. Hydrogen causes serrated flow in a temperature range bounded by a lower critical temperature which was strain rate dependent and an upper critical temperature which was independent of strain rate.

2. The activation enthalpies which characterize the strain rate dependent lower critical temperature, 0.57 eV at low $\dot{\varepsilon}$ and 0.25 eV at high $\dot{\varepsilon}$, differ significantly from the activation enthalpy for lattice diffusion of H, 0.41 eV. These values can be rationalized on the basis of a model in which the serrated yielding is caused by H atoms at the core of the dislocations. The low strain rate behavior is controlled by diffusion of hydrogen in the hydride at the dislocation core and the high strain rate behavior by the dislocation core diffusion of H.

3. The strain rate independent upper critical temperature cannot be accounted for by a process which is dependent on H diffusion but is consistent with the dislocation core hydride model in which it corresponds to the solvus temperature of the dislocation core hydride.

4. Carbon solutes have only a small effect on the hydrogen controlled serrated flow.

5. Serrated flow due to C solutes was observed and the results are in good agreement with previous studies. The serrated flow caused by C is not affected by the presence of H in solution.

ACKNOWLEDGEMENTS

This work was supported by the Office of Naval Research Grant N00014-83-K-0468.

REFERENCES

1. J.P. Hirth and J. Lothe, *Theory of Dislocations*, McGraw-Hill, New York, p 621 (1967).
2. F.R.N. Nabarro, *Theory of Crystal Dislocations*, Oxford U. Press, Oxford, p. 458 (1967).
3. S. Kinoshita, J.P. Wray and G.T. Horne, *Trans. AIME* **233**, 1902 (1965).
4. H. Yoshinaga, K. Toma, K. Abe and S. Morozumi, *Phil. Mag.*, **23**, 1387 (1971).
5. B. Rassell, *Phil. Mag.*, **8**, 615 (1963).
6. B.J. Brindley and P.J. Worthington, *Acta Metall.*, **17**, 1357 (1969).
7. J.W. Edingotn and R.E. Smallman, *Acta Metall.*, **12**, 1313 (1964).
8. G.F. Bolling, *Phil. Mag.*, **4**, 537 (1959).
9. A.H. Cottrell, Vacancies and other point defects in metal and alloys, *Inst. Metals*, London, p1 (1958).
10. Y. Nakada and A.S. Keh, *Acta Metall.*, **18**, 437 (1970).
11. T. Boniszewski and GT.C. Smith, *Acta Metall.*, **11**, 165 (1963).
12. B.A. Wilcox and G.C. Smith, *Acta Metall.*, **12**, 371 (1964).
13. A.H. Windle and G.C. Smith, *Metal Science Journal*, **4**, 136 (1970).
14. J.S. Blakemore, *Metall. Trans.*, **1**, 145 (1970).
15. J.S. Blakemore, *Metall. Trans.*, **1**, 151 (1970).
16. W.M. Robertson, Z. Metallk., **64**, 436 (1973).
17. F.R.N. Nabarro, Report on the Strength of Solids, *The Physical Society*, London **38** (1948).
18. A.H. Cottrell, *Phil. Mag.*, **44**, 829 (1953).

19. R. Kirchheim, *Acta Metall.* **29**, 845 (1981).

20. T.B. Flanagan, N.B. Mason and H.K. Birnbaum, *Scripta Metall.* **15**, 109 (1981).

Table I. Chemical Analysis of the Specimen Material
(all concentrations are in at ppm)

	H	C	O	N	S
Ni	< 5	39	25	4	ND
Ni-H	270	44	29	4	ND
Ni-C	< 5	5096	51	4	ND
Ni-C-H	266	5047	55	4	ND

FIGURE CAPTIONS

Figure 1. Typical segments of the stress strain curves of the Ni-270 at ppm H alloys at a strain rate of 1.8×10^{-6} s^{-1} (A) and 4.4×10^{-5} s^{-1} (B) at temperatures near the lower critical temperature.

Figure 2. Typical segments of the stress-strain curves of the Ni-270 at ppm H alloys at a strain rate of 1.2×10^{-5} s^{-1} (A,C) and 4.4×10^{-4} s^{-1} (B) at temperatures near the upper critical temperature.

Figure 3. Typical segments of the stress-strain curves of the Ni-270 at ppm H alloys at a strain rate of 1.8×10^{-6} s^{-1} (Top) and 2.8×10^{-7} s^{-1} (bottom) at temperatures near the upper critical temperature. Some of the load discontinuities at $\dot{\varepsilon} = 1.8 \times 10^{-7}$ s^{-1}, such as those shown at 228k, are the result of instrumental artifacts. These were present only at the lowest strain rate.

Figure 4. Temperature-strain rate diagram for the region of serrated flow in Ni-270 at ppm H alloys. ● indicate tests where no serrations were seen. ○ indicate tests which exhibited serrated flow.

Figure 5. Temperature-strain rate diagram for the region of serrated flow in the Ni-5100 at ppm C alloy. The previous data by Nakoda et al. (Ref. 10) are shown by the broken lines. ● indicates tests which did not exhibit serrations and ○ indicates tests which had serrated flow.

Figure 6. Typical segments of the stress-strain curves of the Ni-5050 at ppm C - 270 at ppm H alloy at a strain rate of 4.4×10^{-5} s^{-1} at temperatures between 228 K and 254 K.

Figure 7. Temperature-strain rate diagram for the region of serrated flow in the Ni-5050 at ppm C - 270 at ppm H alloy (—), in the Ni-5100 at ppm C alloy (— • —) and in the Ni-270 at ppm H alloy (-----).

Figure 8. Work-hardening rates of Ni (●), Ni-H (○), Ni-C (▲) and (Ni-C-H (Δ) alloys at a strain rate of 4.1 x 10-5 s-1 at 77, 198 and 295 K. Error bars indicate the range of data from repeated tests.

Figure 9. Effect of H outgassing on the flow curves of Ni (····) and Ni-H (——) alloys strained at 295 K and at 198K at $\dot{\varepsilon} = 4.1 \times 10^{-5}$ s^{-1}. (The abscissa was shifted for the 198 K data for clarity.) After about 10% strain (✱) the specimens were outgassed at 473 K in vacuum for 2 hrs.

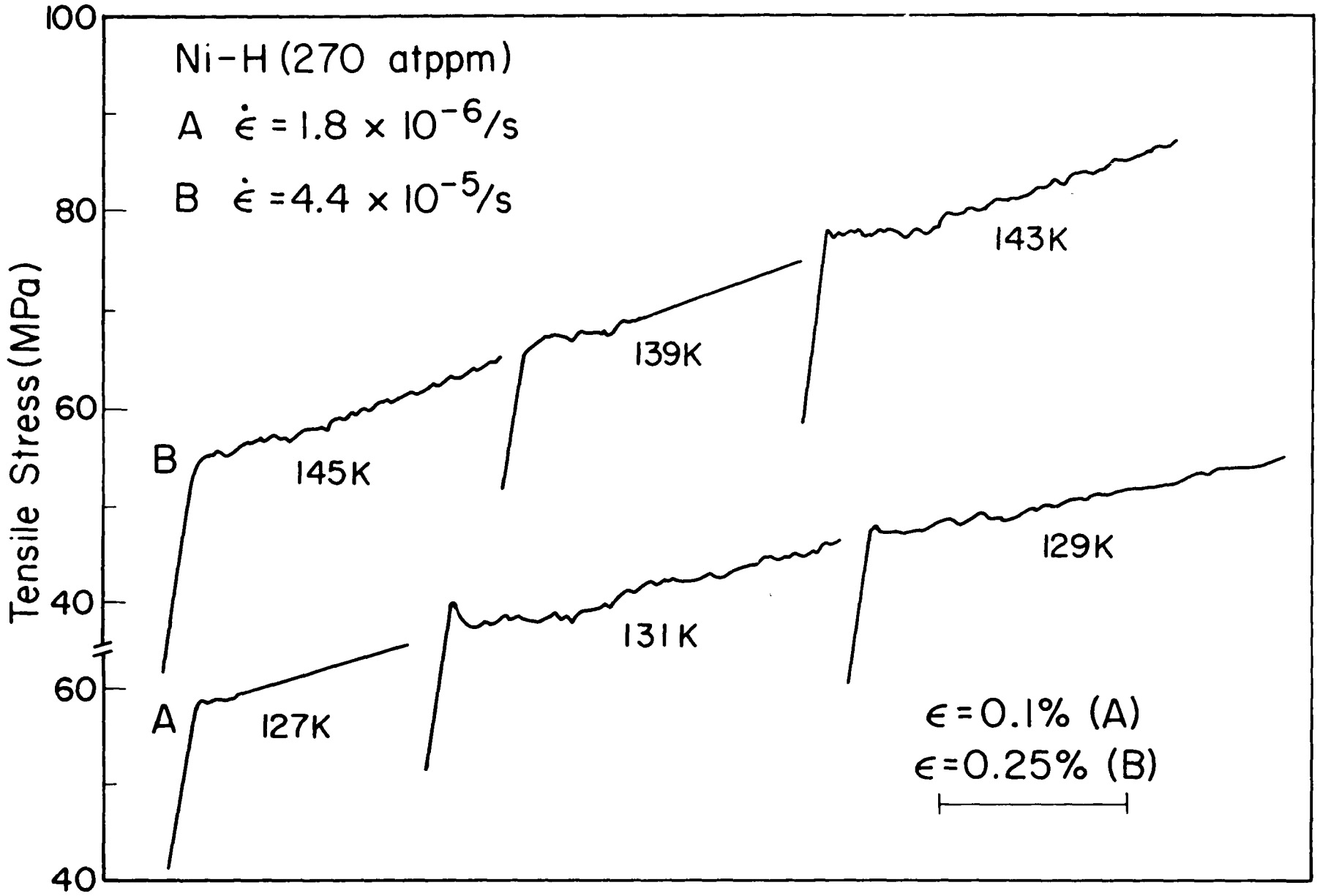
Ni-H (270 atppm)
A $\dot{\epsilon} = 1.8 \times 10^{-6}$/s
B $\dot{\epsilon} = 4.4 \times 10^{-5}$/s
Tensile Stress (MPa)
100
80
60
40
60
40
B
145K
139K
143K
A
127K
131K
129K
ϵ = 0.1% (A)
ϵ = 0.25% (B)

Fig. 1

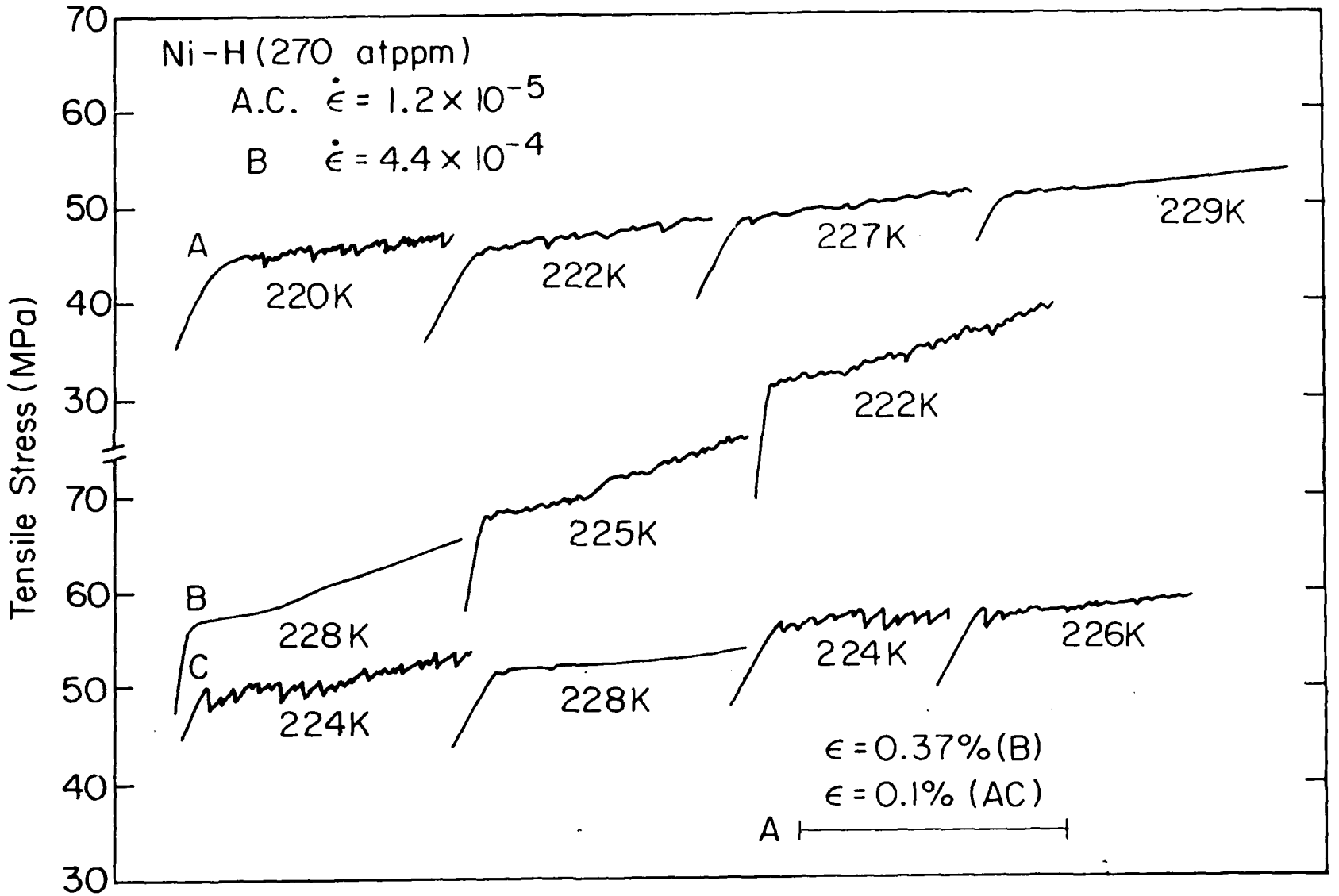
Ni-H (270 atppm)
A.C. $\dot{\epsilon} = 1.2 \times 10^{-5}$
B $\dot{\epsilon} = 4.4 \times 10^{-4}$
Tensile Stress (MPa)
70
60
50
40
30
70
60
50
40
30
A
220K
222K
227K
229K
222K
225K
B
228K
C
224K
228K
224K
226K
$\epsilon = 0.37\%$ (B)
$\epsilon = 0.1\%$ (AC)
A

Fig. ②

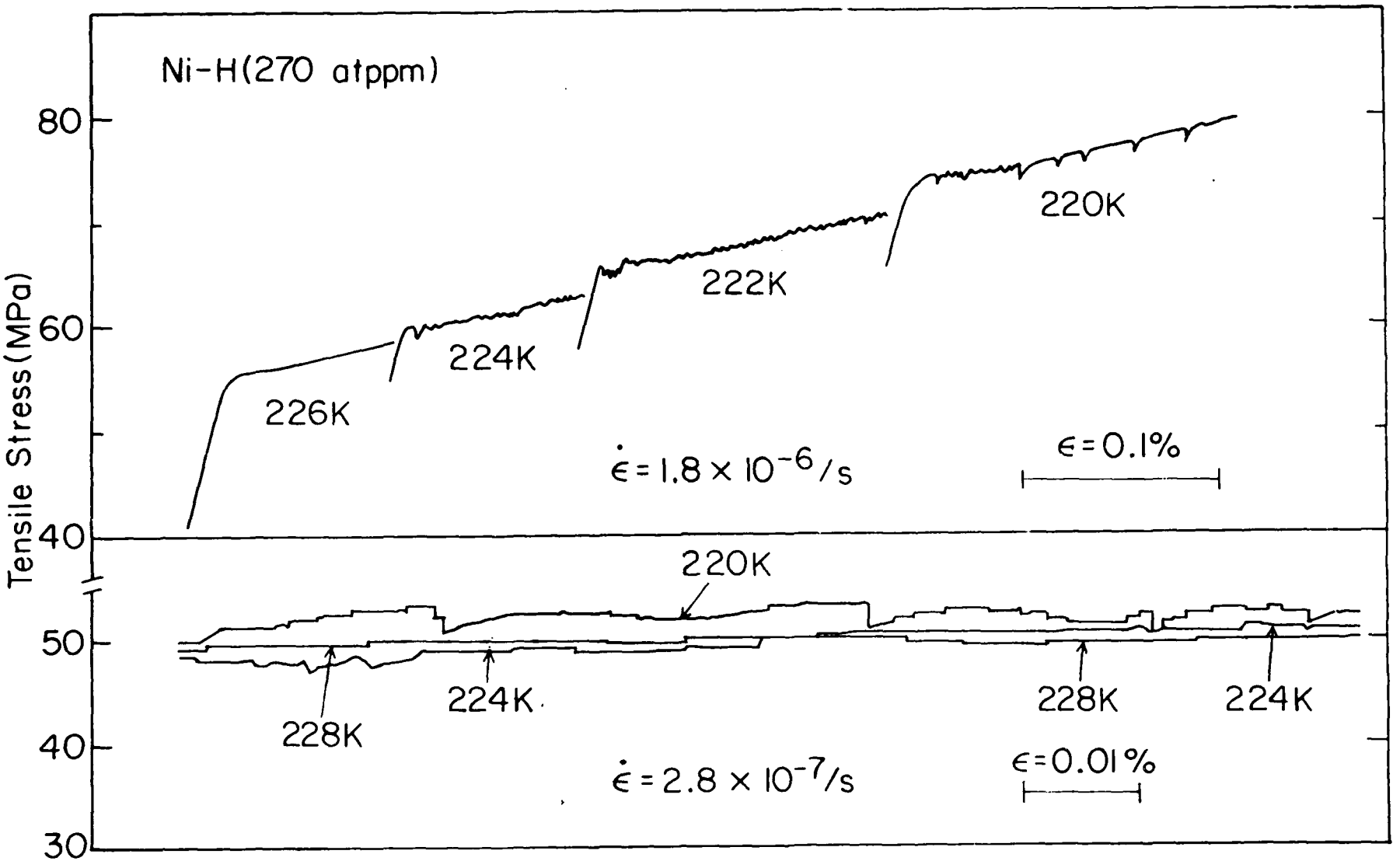
Ni-H(270 atppm)
Tensile Stress (MPa)
80
60
40
50
40
30
226K
224K
222K
220K
$\dot{\epsilon} = 1.8 \times 10^{-6}/s$
$\epsilon = 0.1\%$
220K
228K
224K
228K
224K
$\dot{\epsilon} = 2.8 \times 10^{-7}/s$
$\epsilon = 0.01\%$

Fig. 3

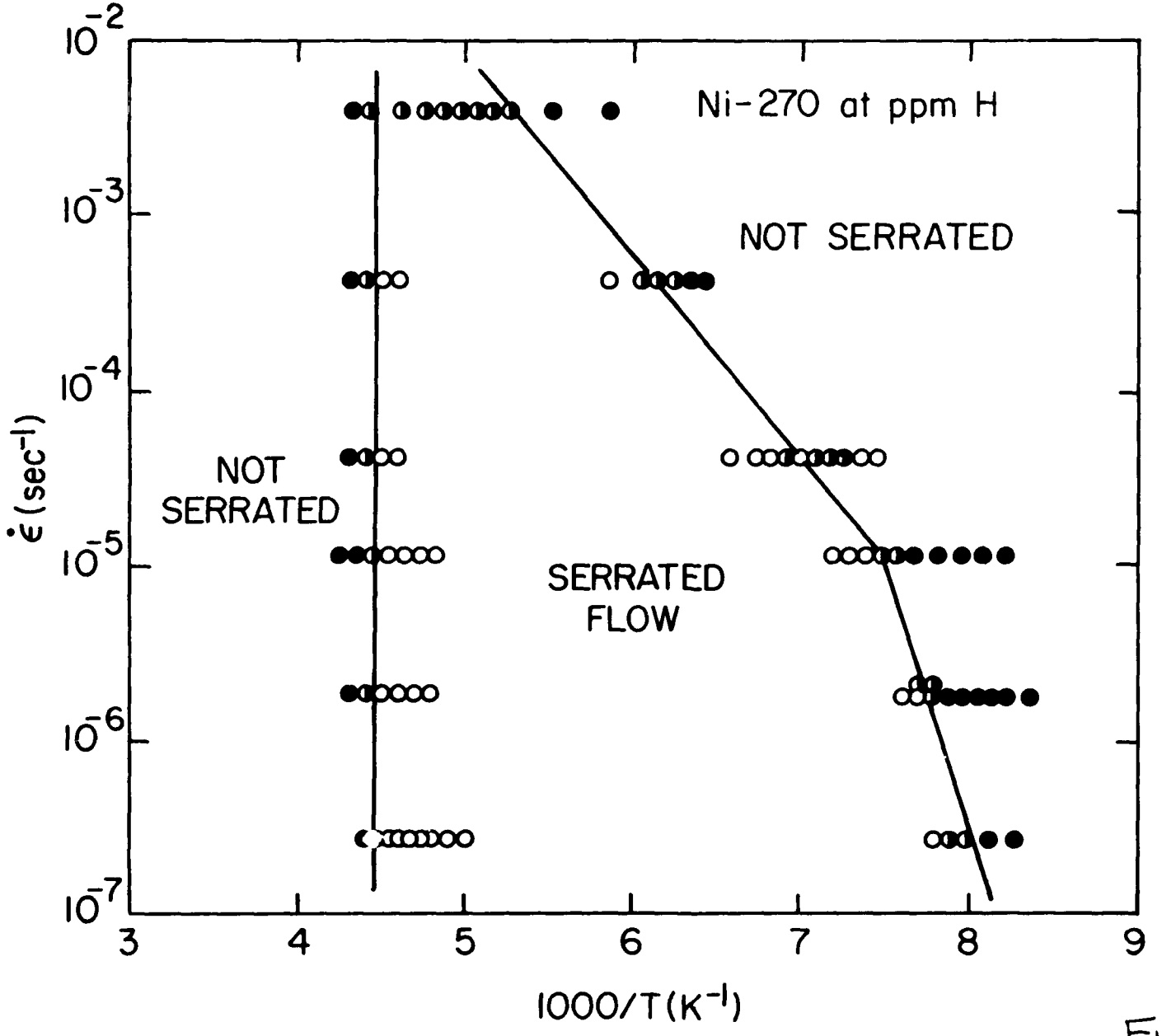
Ni-270 at ppm H
NOT SERRATED
NOT SERRATED
SERRATED FLOW
$\dot{\epsilon}$ (sec^{-1})
10^{-2}
10^{-3}
10^{-4}
10^{-5}
10^{-6}
10^{-7}
3
4
5
6
7
8
9
1000/T(K^{-1})

Fig. 4

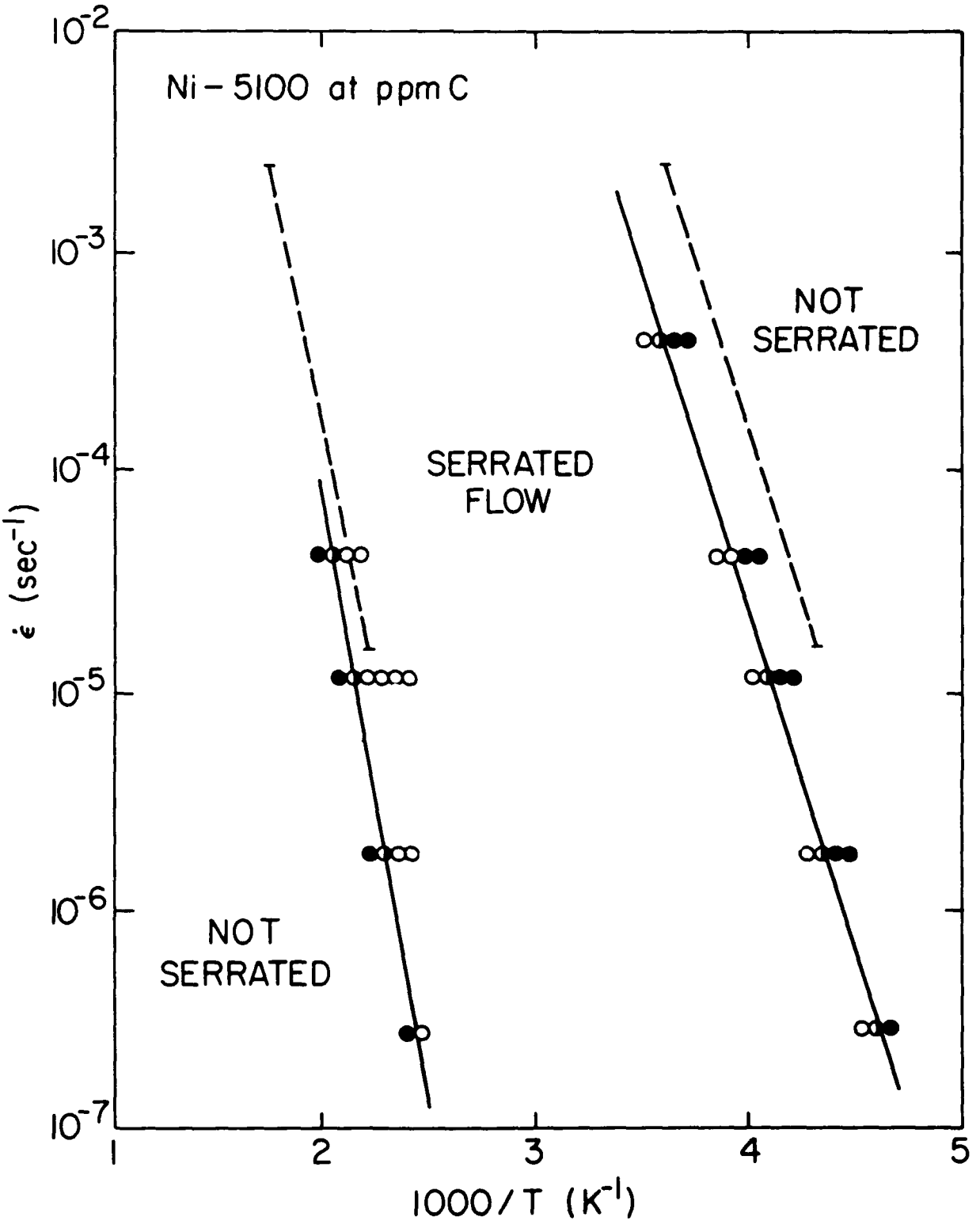
Ni – 5100 at ppm C
NOT SERRATED
SERRATED FLOW
NOT SERRATED
$\dot{\epsilon}$ (sec^{-1})
10^{-2}
10^{-3}
10^{-4}
10^{-5}
10^{-6}
10^{-7}
1
2
3
4
5
1000 / T (K^{-1})

Fig. 5

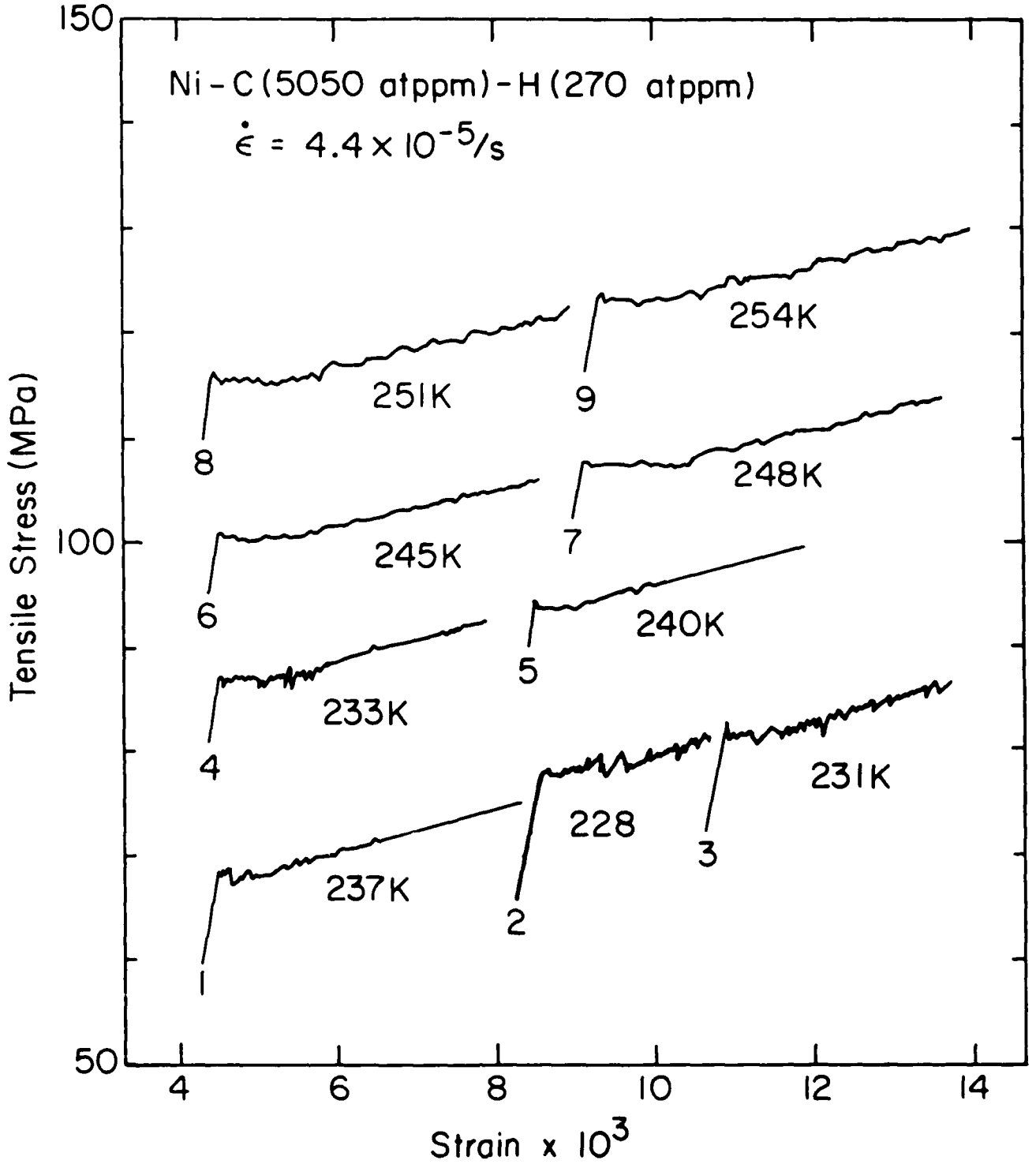
Ni - C (5050 atppm) - H (270 atppm)
$\dot{\epsilon}$ = 4.4 x 10^{-5}/s
Tensile Stress (MPa)
150
100
50
4
6
8
10
12
14
Strain x 10^3
254K
251K
248K
245K
240K
233K
231K
228
237K
1
2
3
4
5
6
7
8
9

Fig. 6

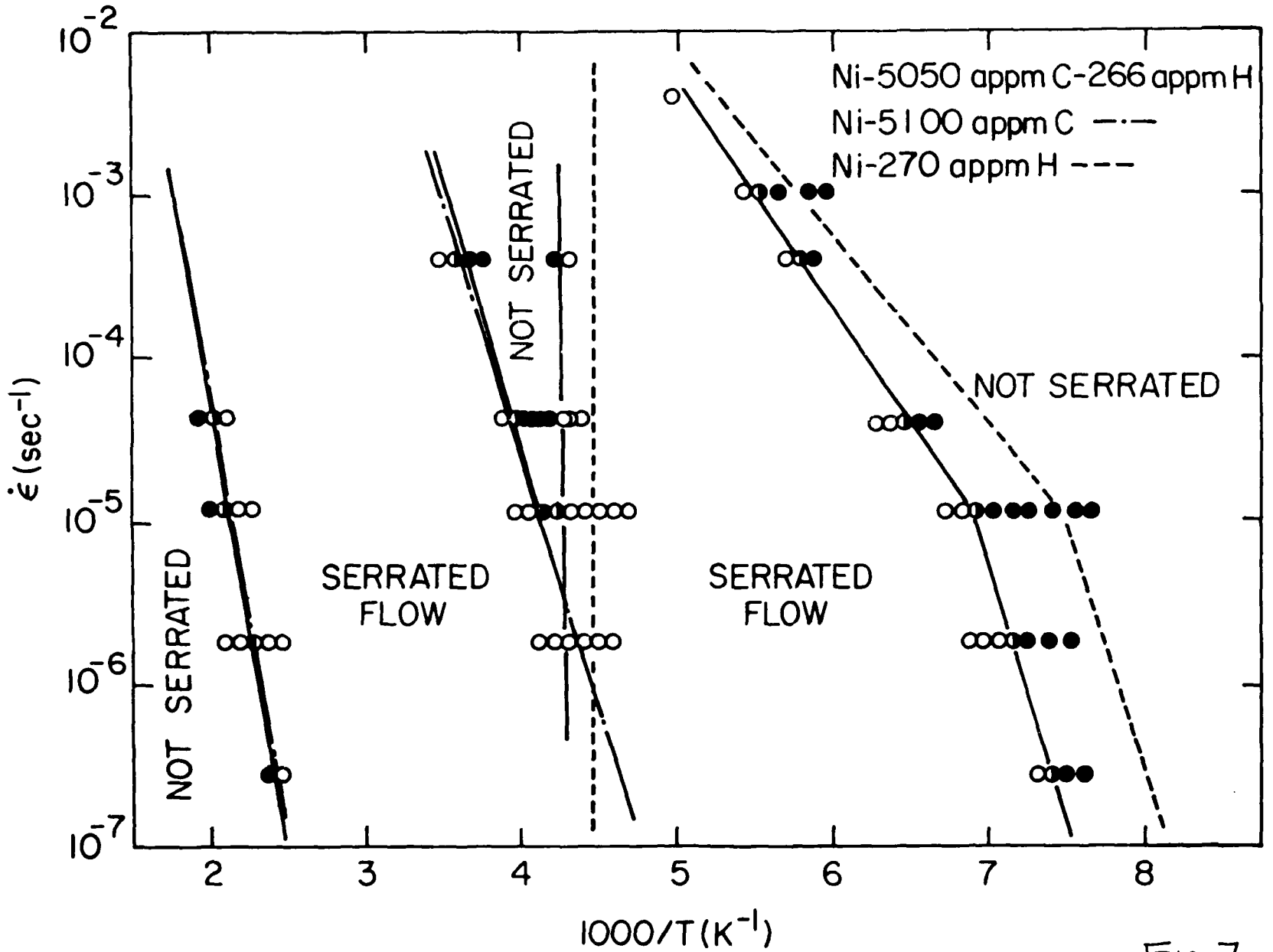
Ni-5050 appm C-266 appm H
Ni-5100 appm C
Ni-270 appm H
NOT SERRATED
SERRATED FLOW
NOT SERRATED
SERRATED FLOW
NOT SERRATED
$\dot{\epsilon}$ (sec^{-1})
10^{-2}
10^{-3}
10^{-4}
10^{-5}
10^{-6}
10^{-7}
2
3
4
5
6
7
8
1000/T(K^{-1})

Fig. 7

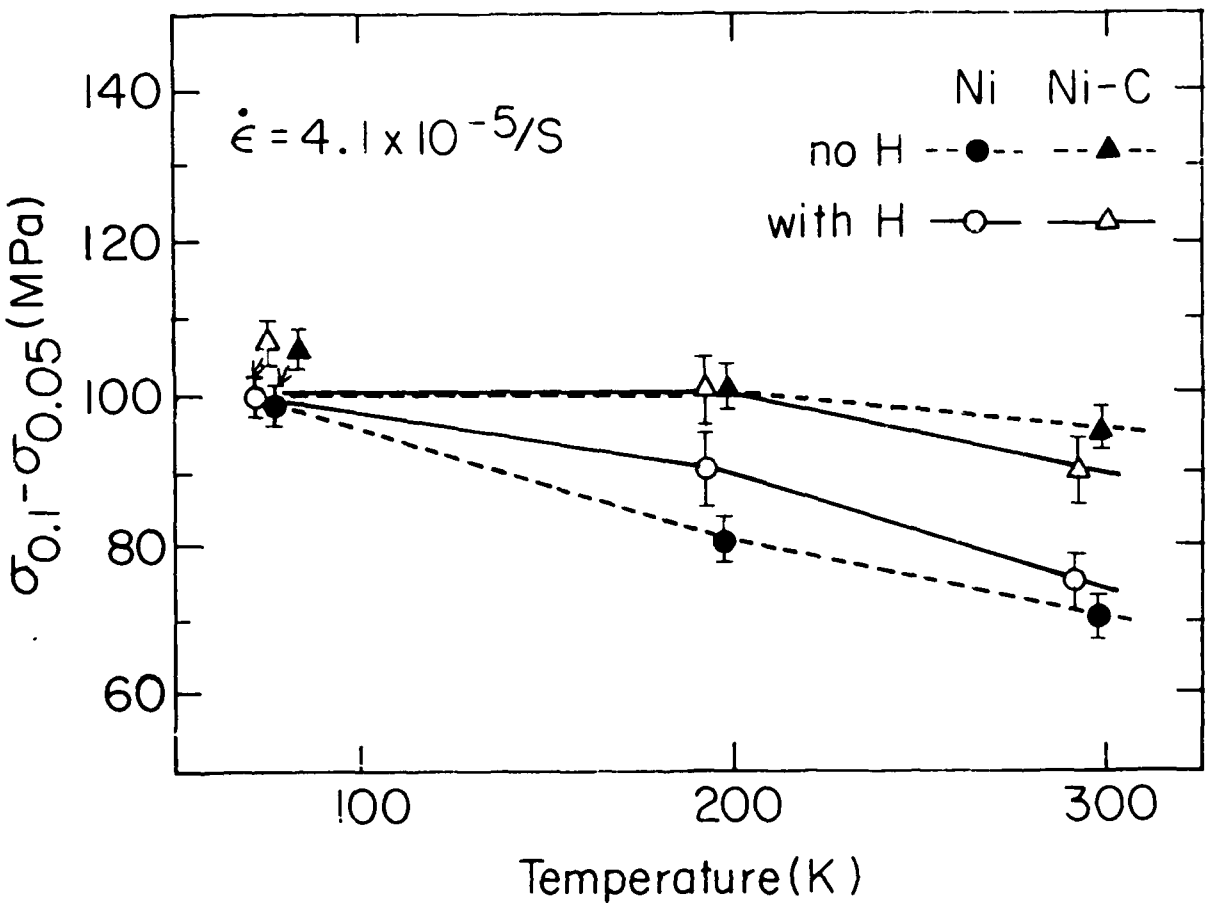
$\dot{\epsilon} = 4.1 \times 10^{-5}/S$
Ni Ni-C
no H
with H
140
120
100
80
60
$\sigma_{0.1} - \sigma_{0.05}$ (MPa)
100
200
300
Temperature (K)

Fig. ⑧

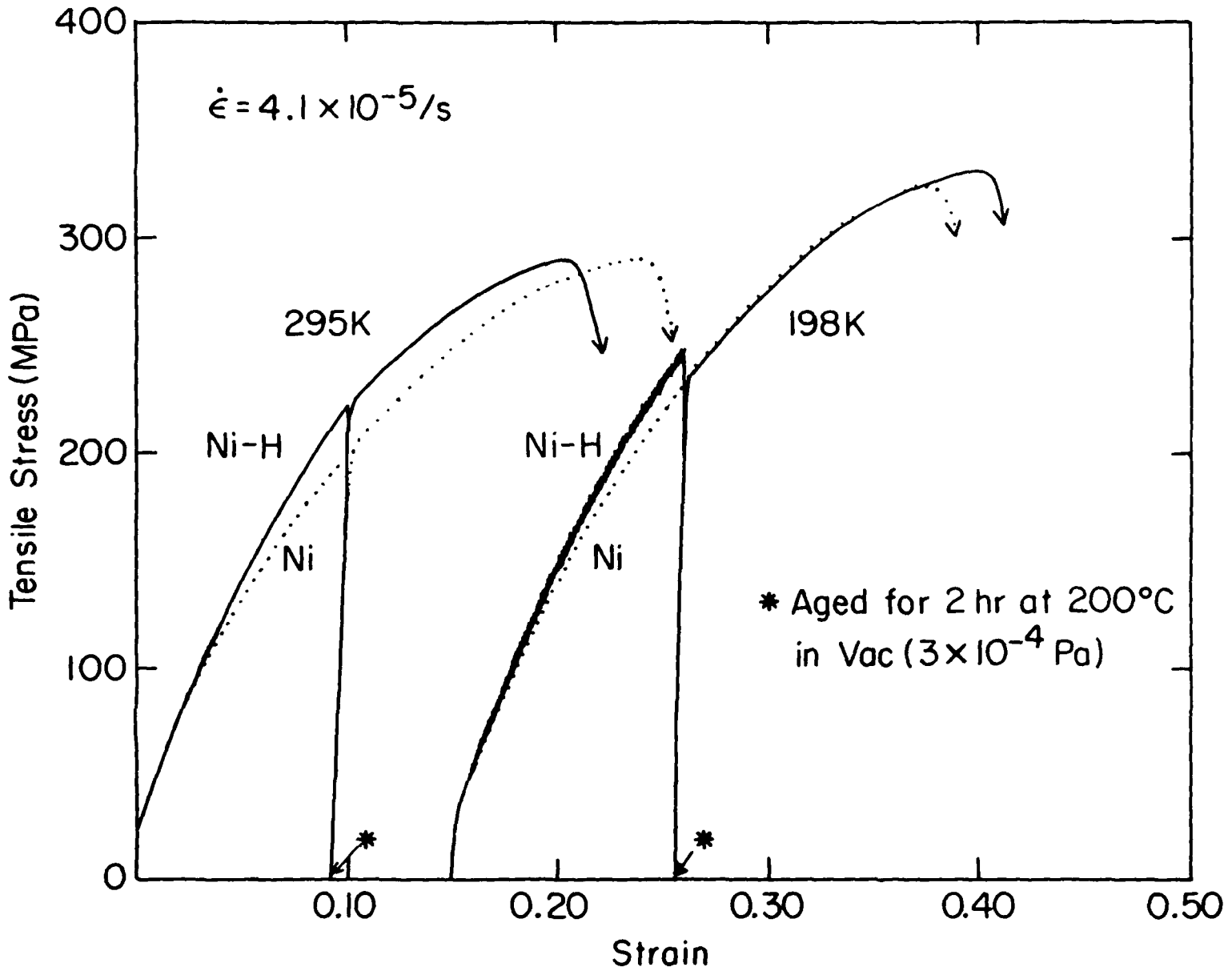
400
300
200
100
0
$\dot{\epsilon} = 4.1 \times 10^{-5}/s$
295K
198K
Ni-H
Ni
Ni-H
Ni
* Aged for 2 hr at 200°C
in Vac (3×10^{-4} Pa)
Tensile Stress (MPa)
0.10
0.20
0.30
0.40
0.50
Strain

Fig. 9